Microwave-Optical Mixing in $LiNbO_3$ Modulators

Ganesh K. Gopalakrishnan, *Member, IEEE,* William K. Burns, *Member, IEEE,* and Catherine H. Bulmer

Abstract—**An investigative study of microwave-optical mixing in different configurations of $LiNbO_3$ Mach-Zehnder interferometric modulators is presented. In each case, models that describe mixer performance are developed and are shown to be in good agreement with measurements. For antenna remoting applications, a technique to down-convert RF signals is demonstrated by cascading in series a pair of Mach–Zehnder interferometric modulators. In general, it is shown that by virtue of their truly broad-band characteristics, interferometric modulators can also be employed as microwave mixers at frequencies up to 40 GHz.**

I. Introduction

RECENT advances in optoelectronic technology have rendered multi-gigahertz bandwidth fiberoptic systems practical. As efforts to enhance the bandwidth of these systems continue to grow, so does the demand for broadband optical sources. Recently, some ultra-broadband, low half-wave voltage (V_π) Ti:$LiNbO_3$ Mach–Zehnder interferometric external modulators have been reported [1]–[3]. In these devices, the optical carrier is modulated by applying an RF electrical drive signal to the modulator. Modulation occurs via electrooptic mixing of the optical carrier with the RF-drive signal. Hence, Mach–Zehnder interferometric modulators could be fundamentally viewed as electro-optic mixers [4] and can be applied to modulate and mix RF signals. Whereas the topic of RF modulation with interferometric modulators has received a lot of attention, the potential of these devices to mix and down-convert RF signals has not yet been explored. Interferometric modulators, by virtue of their truly broadband characteristics, can also be applied to down-convert RF signals at frequencies extending well into the millimeter-wave spectrum, to a lower intermediate frequency (IF). In this research, we investigate theoretically and experimentally RF modulation and mixing as they occur in different configurations of Mach–Zehnder interferometric modulators.

This paper is organized as follows: in Section II, we present RF characteristics of the two traveling wave modulators considered in this research; in Section III, we investigate intermodulation distortion (IMD) and compression in a single Mach–Zehnder interferometer biased at quadrature; in Section IV, we bias the modulator for maximum transmission and investigate down-conversion of RF to an IF; in Section V, we present a novel integrated-optic mixer by cascading in series a pair of interferometric modulators biased at quadrature; Section VI is devoted to discussions, and finally the conclusions are presented in Section VII.

Although the modulators considered in this research perform very well to 40 GHz, we were limited in our mixing experiments to less than 18 GHz due to equipment limitations. Hence, in each configuration, the actual mixing experiments were performed at a frequency centered around 15.5 GHz and the data obtained is compared with theory. The theoretical analysis is then extended to 40 GHz to obtain the projected response.

II. Modulator Performance

Central to broadband operation of an electro-optic modulator are two key factors: microwave-optical velocity match and electrical leakage to substrate modes. In $LiNbO_3$, traveling wave (TW) modulators, the microwave and optical signals typically travel at different velocities thereby limiting device bandwidth. Whereas the velocity of the optical wave (determined by the index of the guided optical mode) is fixed, the microwave velocity can be engineered to nearly match that of the optical wave by employing thick coplanar electrodes [5]. Electrical leakage to substrate modes is caused by an anomalous phase-matched coupling of electrical power from the guided coplanar mode to dielectric substrate modes of $LiNbO_3$. This problem can be eliminated at a given frequency by appropriate choice of substrate thickness [6]. For the devices reported here, microwave-optical velocity match was nearly achieved by employing thick (≥ 15 μm) coplanar electrodes and electrical leakage to substrate modes was eliminated by thinning the substrate. The devices (designated MZ1 and MZ2) were fabricated on z-cut $LiNbO_3$ substrates coated with a 0.9 μm SiO_2 buffer layer. The center strip width of the coplanar waveguide (CPW) electrode was 8 μm, gapwidths were 15 μm, ground planes were 2–3 mm wide, and the electrode interaction length was 24 mm. The devices were designed for operation at an optical wavelength of 1.3 μm with the characteristic impedance of the CPW line (Z_D) in the active section being approximately 35 Ω. MZ1 and MZ2 were fabricated on substrates 0.2 and 0.15 mm thick, respectively, and the substrates were 8 mm wide. The average gold electrode

Manuscript received March 17, 1993; revised June 9, 1993. This work was funded by the Office of Naval Research Electrooptics block program.

G. K. Gopalakrishnan is with Maryland Advanced Development Laboratory, at the Naval Research Laboratory, Code 5671, Washington, DC 20375.

W. K. Burns and C. H. Bulmer are with the Naval Research Laboratory, Code 5671, Washington, DC 20375.

IEEE Log Number 9212956.

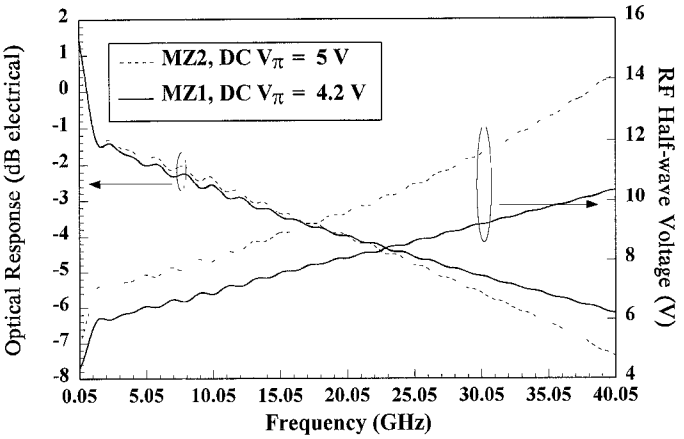

Fig. 1. RF performance characteristics of MZ1 and MZ2.

thicknesses of MZ1 and MZ2 were 15 and 18 μm with the DC V_π's being 4.2 and 5 V, respectively. When biased for maximum transmission, the optical insertion loss through each device was approximately 4 dB.

From a fit to the electrical response of the modulator comprising conductor, dielectric and radiative losses [7] and considering the microwave-optical index mismatch (0.06 for MZ1 and 0.128 for MZ2) obtained from a fit to the optical response, the modeled optical responses of the devices are shown in Fig. 1. The model [7] also takes into consideration reflections that occur at the transition from the 35 Ω CPW line to the 50 Ω load. Here, our primary interest is to characterize traveling wave modulators in terms of their mixing efficiency. A fundamental mixer parameter that reflects mixing efficiency is its RF conversion loss. As will be evident later in this paper, the RF half-wave voltage ($V_\pi(f)$) of the modulator being proportional to the conversion loss, adequately characterizes the mixing efficiency of the modulator. $V_\pi(f)$ may be obtained from the optical response of the modulator by using the following expression:

$$V_\pi(f) = V_\pi(\mathrm{DC}) \left(\frac{Z_0 + Z_D}{2Z_D}\right) 10^{-\mathrm{OR}/20} \tag{1}$$

where $V_\pi(\mathrm{DC})$ is the half-wave voltage of the modulator at DC, $Z_0 = 50\ \Omega$ is the characteristic impedance of the line, Z_D is the characteristic impedance of the CPW electrode of the device and OR is the optical response of the modulator in dB electrical. Also shown in Fig. 1 are the modeled RF half-wave voltages of MZ1 and MZ2 as a function of frequency. For the analyses to be presented in the ensuing sections of this paper, $V_\pi(f)$ was obtained from Fig. 1.

III. Single Interferometric Modulator Biased at Quadrature

When a Mach–Zehnder interferometer, biased at quadrature, is modulated, a highly modulated optical signal at the modulating signal frequency is generated and even harmonics are suppressed. In this case, the desired IF signal is the modulating RF signal itself. In this mode of operation, the output varies linearly with input as long as the amplitude of the input signal is small compared to V_π. However, if the amplitude of the input becomes comparable to V_π, then compression sets in, and when more than one input signal is present, IMD becomes important. In this section, we examine compression and IMD in a traveling wave modulator biased at quadrature, by applying a two-tone input. Previously [4], a similar investigation was done at a low frequency ($\approx$2 GHz). Here, our experimental investigations are centered at 15.5 GHz. We also develop a model based on $V_\pi(f)$ to evaluate modulator performance and demonstrate excellent agreement with measured data. The analysis is then extended to 40 GHz and results are presented.

A. Theory

For a Mach–Zehnder interferometer, the output optical power at the photodetector P_0 in terms of the input-optical power into interferometer P_{in} may be represented as

$$P_0 = \frac{T_D P_{\mathrm{in}}}{2}(1 + \cos[\phi_0 + \Delta\phi]) \tag{2}$$

where ϕ_0 is the DC phase bias (= 90° when biased at quadrature), T_D represents the coupling and optical transmission losses of the link with the interferometer biased for maximum transmission, and $\Delta\phi$ is the phase shift due to application of an ac signal. For an input sinusoidal signal at an angular frequency ω, $\Delta\phi$ is given by:

$$\Delta\phi = \frac{\pi V}{V_\pi} M(\omega) \sin(\omega t + \theta(\omega)) \tag{3}$$

where V is the amplitude of the input ac signal, $M(\omega)$ is the magnitude of the normalized frequency response of the modulator, and $\theta(\omega)$ is its phase response. $\theta(\omega)$ is representative of the delay in the modulated signal due to microwave-optical velocity mismatch. To study high-frequency mixing in TW modulators, the frequency dependent roll-off in the modulator's RF response should be taken into consideration. Since the frequency dependent roll-off tends to increase the half-wave voltage of the modulator, we assign frequency dependence to the half-wave voltage and obtain

$$\Delta\phi = \frac{\pi V}{V_\pi(\omega)} \sin(\omega t + \theta(\omega)) \tag{4}$$

where $V_\pi(\omega)$ is the RF half-wave voltage of the modulator. When the modulator is biased at quadrature, ϕ_0 = 90° and we have:

$$P_0 = \frac{T_D P_{\mathrm{in}}}{2}\left(1 - \sin\left[\frac{\pi V}{V_\pi(\omega)} \sin(\omega t + \theta(\omega))\right]\right). \tag{5}$$

Whereas the above equation corresponds to a single tone input, for two tone inputs of amplitudes V_1 and V_2 at an-

gular frequencies ω_1 and ω_2, we have

$$P_0 = \frac{T_D P_{in}}{2}\left(1 - \sin\left[\frac{\pi V_1}{V_\pi(\omega_1)}\sin(\omega_1 t + \theta(\omega_1)) + \frac{\pi V_2}{V_\pi(\omega_2)}\sin(\omega_2 t + \theta(\omega_2))\right]\right). \quad (6)$$

Expanding the above equation in terms of Bessel functions and dropping third and higher order terms, we get:

$$\begin{aligned} P_0 = \frac{T_D P_{in}}{2}\,(1 &- 2J_1(X_1)J_0(X_2)\sin[\omega_1 t + \theta(\omega_1)] \\ &- 2J_0(X_1)J_1(X_2)\sin[\omega_2 t + \theta(\omega_2)] \\ &- 2J_1(X_1)J_2(X_2)\sin[(\omega_1 - 2\omega_2)t \\ &+ \theta(\omega_1) - 2\theta(\omega_2)] \\ &- 2J_1(X_1)J_2(X_2)\sin[(\omega_1 + 2\omega_2)t \\ &+ \theta(\omega_1) + 2\theta(\omega_2)] \\ &- 2J_2(X_1)J_1(X_2)\sin[(\omega_2 - 2\omega_1) \\ &+ \theta(\omega_2) - 2\theta(\omega_1)] \\ &- 2J_2(X_1)J_1(X_2)\sin[(\omega_2 + 2\omega_1)t \\ &+ \theta(\omega_2) + 2\theta(\omega_1)]) \end{aligned} \quad (7)$$

where J_n is the Bessel function of order n, $X_1 = \pi V_1/V_\pi(\omega_1)$ and $X_2 = \pi V_2/V_\pi(\omega_2)$. In the above equation, the contribution of the DC term (P_{DC}) to the optical power at the photodetector is given by $P_{DC} = T_D P_{in}/2$. If R is the responsivity of the photodetector, then the detected DC photocurrent $I_{DC} = RT_D P_{in}/2$. At angular frequencies ω_1, ω_2, $2\omega_1 - \omega_2$, and $2\omega_2 - \omega_1$, the electrical powers delivered to a 50 Ω load may then be evaluated using the following expressions:

$$P(\omega_1) = L(\omega_1)\frac{I_{DC}^2}{2}(2J_1(X_1)J_0(X_2))^2 \cdot 50 \quad (8)$$

$$P(\omega_2) = L(\omega_2)\frac{I_{DC}^2}{2}(2J_0(X_1)J_1(X_2))^2 \cdot 50 \quad (9)$$

$$P(2\omega_1 - \omega_2) = L(2\omega_1 - \omega_2)\frac{I_{DC}^2}{2}(2J_2(X_1)J_1(X_2))^2 \cdot 50 \quad (10)$$

$$P(2\omega_2 - \omega_2) = L(2\omega_2 - \omega_1)\frac{I_{DC}^2}{2}(2J_1(X_1)J_2(X_2))^2 \cdot 50. \quad (11)$$

Here, $L(\omega)$ collectively represents frequency dependent losses such as detector roll-off and cable losses that limit the performance of the fiber-optic link. At sufficiently high frequencies, $L(\omega)$ could become significant and, hence, must be taken into consideration to evaluate link performance. From the above equation, it can be seen that signal powers at different frequencies are directly proportional to the arguments (X_1, X_2) of the Bessel function and, hence, are inversely proportional to $V_\pi(\omega)$. Thus, with other conditions remaining the same, a smaller $V_\pi(\omega)$ means a larger modulated signal strength.

B. Experiments

The results reported in this section correspond to modulator MZ1. Illustrated in Fig. 2 is a block diagram of the experimental setup. Two synthesized sources operating at frequencies f_1 and f_2 are power combined and the two-tone input is applied to one port of the modulator while the other port is terminated in a 50 Ω load. The two amplifiers provide the input-drive power necessary to carry out the experiments. The photodetector used here was a GTE InGaAs detector (responsivity = 0.5 A/W) whose 3 dB bandwidth was approximately 20 GHz. Based on the theoretical analysis presented above, for an interferometer biased at quadrature, the output power is significant at the signal (f_1, f_2) and third-order intermodulation ($2f_1 \pm f_2$ and $2f_2 \pm f_1$) frequencies. If $f_1 \approx f_2$, then the third-order frequencies are only $f_2 - f_1$ away from signal frequencies, and appear as spurious signals in the RF passband and, hence, cannot be filtered out. Also, these signals being proportional to the cube of input power rise rapidly with input power, thereby limiting the dynamic range of the modulator. To investigate this, two equal amplitude signals ($V_1 = V_2$) at frequencies $f_1 = 15.52$ GHz and $f_2 = 15.56$ GHz, were power combined and applied to the modulator. The output power at the detector was monitored at the signal (15.52 and 15.56 GHz) and third-order (15.48 and 15.6 GHz) frequencies. The RF half-wave voltage of the modulator at these frequencies (determined from Fig. 1) was approximately 7.7 V. Fig. 3(a) shows the variation of detected output power at the signal and third-order frequencies as a function of input RF power applied to the modulator, for a DC photocurrent of 0.4 mA; $L(\omega)$ corresponding to these measurements was approximately −3.5 dB. As shown, the data obtained is in very good agreement with theory. Here, 1 dB compression and third-order intercept points were determined from a curve fit to the data, and were estimated to occur at input powers of approximately 18 and 27 dBm, respectively. Assuming the same DC photocurrent and $L(\omega)$ (= −3.5 dB), we extended our analysis to 40 GHz, and the computed results in this case are shown in Fig. 3(b); the RF half-wave voltage of the modulator at this frequency was 10.4 V. Here, 1 dB compression and third-order intercept points were calculated by extrapolating linear portions of the fundamental and third-order curves, and correspond to input powers of approximately 20.5 and 29.5 dBm, respectively. In actuality, however, at 40 GHz, $L(\omega)$ would be worse than −3.5 dB (due to larger detector roll-off and cable losses at 40 GHz compared to 15.5 GHz) and, therefore, the actual signal strengths would be less than that predicted in Fig. 3(b).

Even though the combination of DC V_π and RF response of this modulator is among the best reported in the literature, it should be obvious from Fig. 3 that the RF

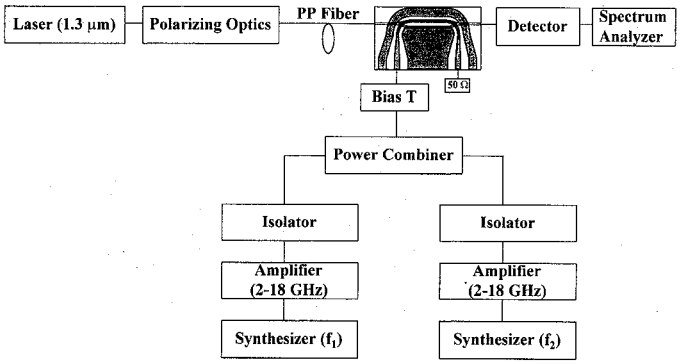

Fig. 2. Block diagram of experimental setup for mixing with a single interferometer.

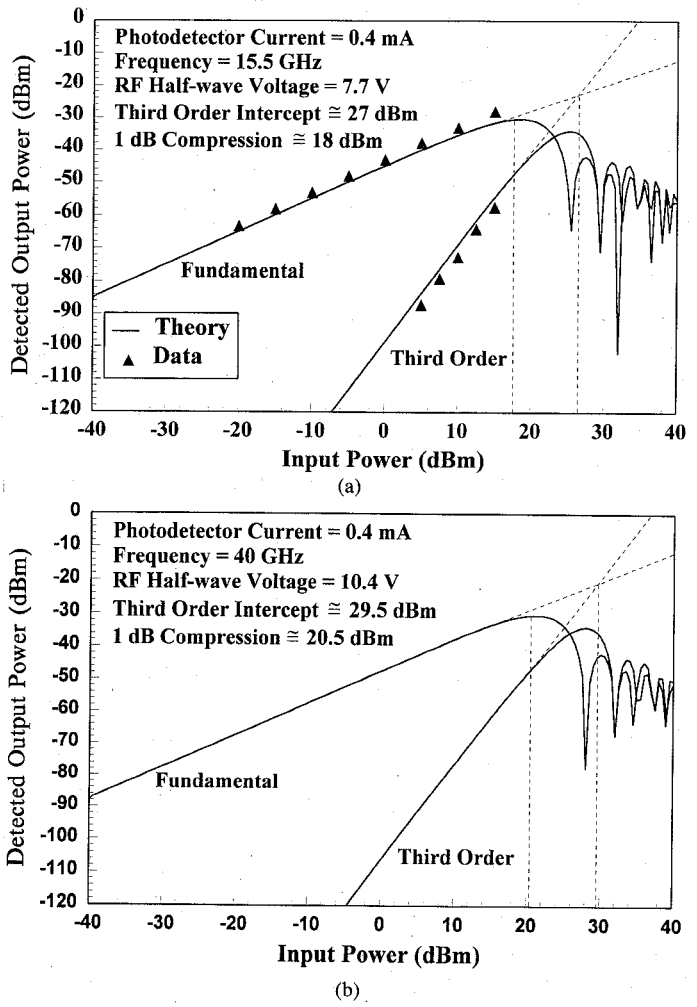

Fig. 3. Fundamental and third-order responses of MZ1 at (a) 15.5 GHz (modeled and measured) and (b) 40 GHz (modeled) for quadrature bias.

conversion loss of the link defined as

RF conversion loss (dB)

$$= \text{detected IF power (dBm)} - \text{input RF power (dBm)} \tag{12}$$

is still very large ($\approx$45 dB at 15.5 GHz and $\approx$48 dB at 40 GHz). The conversion loss at 40 GHz is larger because $V_\pi(f)$ at 40 GHz is larger. This loss can be improved by increasing the laser power and by employing a detector with better responsivity. However, these factors are external to the modulator. From previous analysis, the detected output power and, hence, the conversion loss being inversely proportional to $V_\pi(f)$, can be significantly improved by lowering the $V_\pi(f)$. Although conversion losses comparable to conventional microwave mixers would be very difficult to achieve over a broadband of frequencies, significant improvement in link loss is still possible by lowering $V_\pi(f)$.

IV. Single Interferometric Modulator Biased for Maximum Transmission

The RF transfer characteristics of modulators biased for either maximum ($\phi_0 = 0°$) or minimum ($\phi_0 = 180°$) transmission, closely resemble each other in that the odd harmonics are suppressed. Whereas biasing the modulator for minimum transmission offers the advantages of lower laser noise and smaller optical reflections [8] for the experiments reported in this section, we employed a maximum transmission bias. At this bias, almost all the detected DC optical power is from the guided optical mode itself. For minimum transmission, however, the DC component of power in the guided optical mode is very small and extraneous sources such as scattered light could account for a significant portion of the detected DC optical power. To facilitate accurate comparison of theory with experiments, the DC component of power in the guided optical mode must be known exactly. Therefore, to avoid ambiguities associated with contributions from extraneous sources for minimum transmission bias, we biased our modulator for maximum transmission.

A modulator biased for maximum transmission can be used for RF down-conversion by mixing the low-power RF signal with a larger local oscillator (LO) pump signal. Although the configuration of the experimental set-up in this case is identical to that of the quadrature bias case, there is a functional difference. For a two-tone input applied to a modulator biased at quadrature, the desired IF outputs are the two-tone frequencies themselves. This contrasts with the maximum transmission case, where one of the inputs is actually a single-tone RF signal that is power combined and mixed with a larger LO pump signal (which is the other tone in the quadrature bias case) with the desired IF being the difference between the RF and LO frequencies. Our interest here is to characterize mixer performance for RF down-conversion.

A. Theory

When two signals of amplitudes V_1 and V_2, at angular frequencies ω_1 and ω_2, are applied to a modulator biased for maximum transmission we have

$$P_0 = \frac{T_D P_{\text{in}}}{2}\left(1 + \cos\left[\frac{\pi V_1}{V_\pi(\omega_1)}\sin(\omega_1 t + \theta(\omega_1)) + \frac{\pi V_2}{V_\pi(\omega_2)}\sin(\omega_2 t + \theta(\omega_2))\right]\right). \tag{13}$$

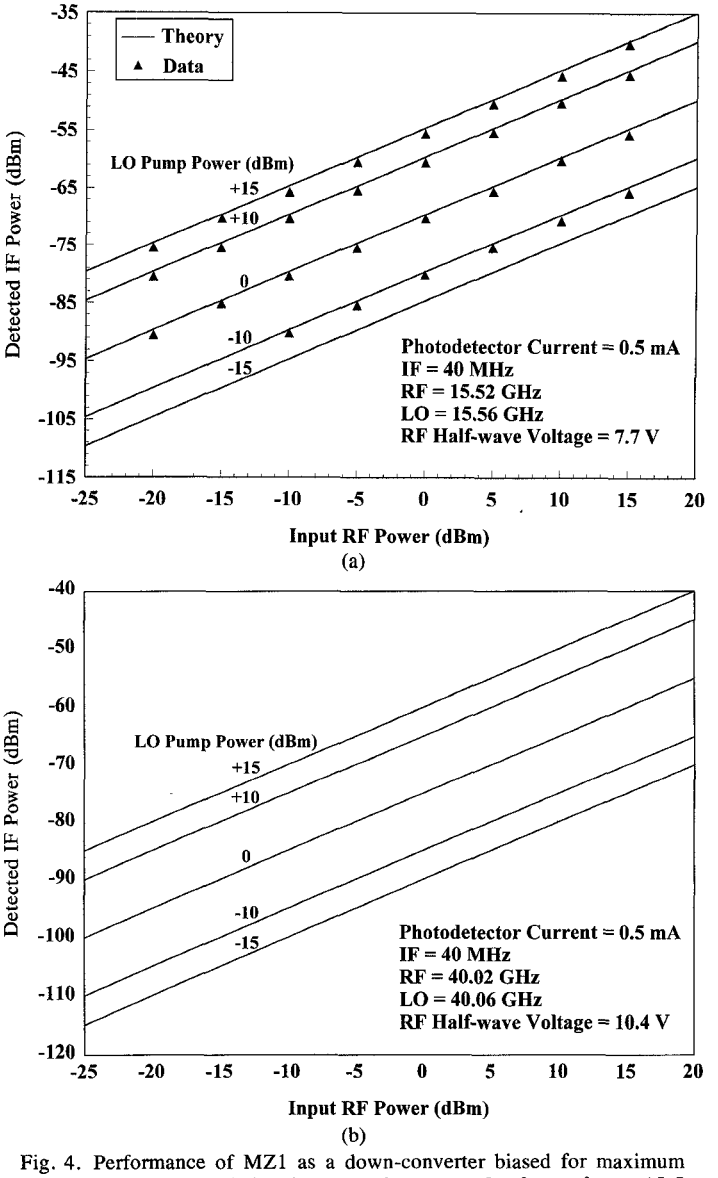

Fig. 4. Performance of MZ1 as a down-converter biased for maximum transmission. (a) Modeled and measured response for $f_{RF} \approx f_{LO} \approx 15.5$ GHz. (b) Modeled response for $f_{RF} \approx f_{LO} \approx 40$ GHz.

Expanding the above equation in terms of Bessel functions and dropping fourth and higher order terms, we get:

$$P_0 = \frac{T_D P_{in}}{2}(1 + J_0(X_1)J_0(X_2) + 2J_2(X_1)J_0(X_2) \cdot \cos[2\omega_1 t + 2\theta(\omega_1)] + 2J_0(X_1)J_2(X_2) \cdot \cos[2\omega_2 t + 2\theta(\omega_2)] - 2J_1(X_1)J_1(X_2)\cos[(\omega_1 - \omega_2)t + \theta(\omega_1) - \theta(\omega_2)] + 2J_1(X_1)J_1(X_2)\cos[(\omega_1 + \omega_2)t + \theta(\omega_1) + \theta(\omega_2)]. \quad (14)$$

From (14), if R is the responsivity of the photodetector, the detected DC photocurrent I_{DC} is given by:

$$I_{DC} = \frac{RT_D P_{in}}{2}(1 + J_0(X_1)J_0(X_2)). \quad (15)$$

At angular frequencies $2\omega_1$, $2\omega_2$, $\omega_1 - \omega_2$ and $\omega_2 + \omega_1$, the electrical powers delivered at a 50 Ω load can be evaluated using the following expressions:

$$P(2\omega_1) = L(2\omega_1)\frac{I_{DC}^2}{2}\left(\frac{2J_2(X_1)J_0(X_2)}{1 + J_0(X_1)J_0(X_2)}\right)^2 \cdot 50 \quad (16)$$

$$P(2\omega_2) = L(2\omega_2)\frac{I_{DC}^2}{2}\left(\frac{2J_0(X_1)J_2(X_2)}{1 + J_0(X_1)J_0(X_2)}\right)^2 \cdot 50 \quad (17)$$

$$P(\omega_1 \mp \omega_2) = L(\omega_1 \mp \omega_2)\frac{I_{DC}^2}{2} \cdot \left(\frac{2J_1(X_1)J_1(X_2)}{1 + J_0(X_1)J_0(X_2)}\right)^2 \cdot 50 \quad (18)$$

B. Experiments

The results reported in this section correspond to modulator MZ1. In this case, the experimental set-up shown

in Fig. 2 is identical to that of the quadrature bias case, except that the modulator was biased for maximum transmission. Two signals at frequencies $f_1 = 15.52$ GHz (RF) and $f_2 = 15.56$ GHz (LO) were power combined and applied to the modulator and the detector power was monitored at the 40 MHz difference frequency. For a detected DC photocurrent of 0.5 mA, Fig. 4(a) shows the variation of detected IF power at 40 MHz with input RF power; the LO pump power varied from -15 to $+15$ dBm. In this measurement, since the IF was at 40 MHz, $L(\omega)$ was very small and hence was neglected. As shown in Fig. 4(a), there is good agreement between theory and experiments. For the range of LO pump and RF input powers shown, the detected IF power increases linearly with both LO and RF powers. However, if the amplitudes of these inputs become comparable with the RF drive voltage, then compression of the detected IF would occur. From Fig. 4(a), when the LO pump power is $+15$ dBm, the conversion loss of the mixer is approximately 56 dB. We extended the analysis to 40 GHz, and the computed results are shown in Fig. 4(b). In this case, the conversion loss for an LO pump power of $+15$ dBm is approximately 60 dB and as before, the conversion loss is larger at 40 GHz since $V_\pi(f)$ is larger at this frequency.

V. Cascaded Interferometric Modulator Pair Biased at Quadrature

In this section, we cascade in series a pair of interferometric modulators biased at quadrature and demonstrate RF down-conversion. This is done by applying a single-tone RF input to one modulator (MZ1) which is then mixed with a larger LO pump signal applied to the other (MZ2). Here, the actual signals that take part in the mixing are optical signals at the RF and LO frequencies, derived from electrical inputs applied to the RF (MZ1) and LO (MZ2) modulators respectively. To efficiently down-convert these to a desired IF, optical signals at both the RF and LO frequencies must be highly modulated, and, hence, to prevent leakage of power to other unwanted frequencies, both modulators should be biased at quadrature. In this configuration, the intended application of the cascaded modulator pair is for antenna remoting. Here, one modulator can be used to transmit the low-power RF signals from a remote location over an optical fiber which can then be down-converted by mixing with a large LO pump signal applied to the other modulator. The tandem arrangement of modulators also allows for multiplication of RF signals applied to each modulator.

A. Theory

Illustrated in a portion of Fig. 5 is the layout of two Mach–Zehnder interferometers (MZ1 and MZ2) cascaded in series. If RF input signals $V_1 \sin \omega_1 t$ and $V_2 \sin \omega_2 t$ are the applied to MZ1 and MZ2, respectively, then P_0 of the pair for quadrature bias is given by:

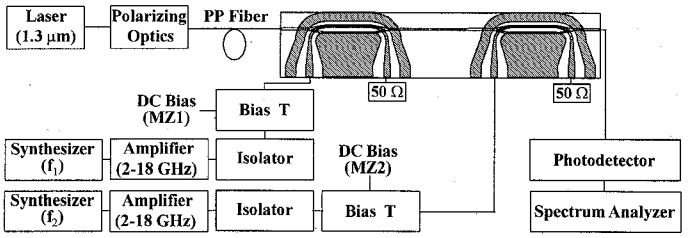

Fig. 5. Block diagram of experimental setup for mixing with cascaded interferometers.

$$P_0 = \frac{T_D P_{\text{in}}}{4}\left(1 - \sin\left[\frac{\pi V_1}{V_{\pi 1}(\omega_1)}\sin(\omega_1 t + \theta(\omega_1))\right]\right) \cdot \left(1 - \sin\left[\frac{\pi V_2}{V_{\pi 2}(\omega_2)}\sin(\omega_2 + \theta(\omega_2))\right]\right) \tag{19}$$

where $V_{\pi 1}(\omega_1)$ and $V_{\pi 2}(\omega_2)$ are the RF half-wave voltages of MZ1 and MZ2 at frequencies ω_1 and ω_2, respectively. Expanding the above equation in terms of Bessel functions and dropping third and higher order terms, we get:

$$\begin{aligned} P_0 = \frac{T_D P_{\text{in}}}{4}\,(1 &- 2J_1(X_1)\sin[\omega_1 t + \theta(\omega_1)] \\ &- 2J_1(X_2)\sin[\omega_2 t + \theta(\omega_2)] \\ &- 2J_1(X_1)J_1(X_2)\sin[(\omega_2 - \omega_1)t + \theta(\omega_2) - \theta(\omega_1)] \\ &- 2J_1(X_1)J_1(X_2)\sin[(\omega_1 + \omega_2)t + \theta(\omega_1) + \theta(\omega_2)] \end{aligned} \tag{20}$$

where $X_1 = \pi V_1 / V_{\pi 1}(\omega_1)$ and $X_2 = \pi V_2 / V_{\pi 2}(\omega_2)$. As before, at angular frequencies ω_1, ω_2, $\omega_1 - \omega_2$ and $\omega_2 + \omega_1$, the electrical powers delivered to a 50 Ω load can be evaluated using the following expressions:

$$P(\omega_1) = L(\omega_1)\frac{I_{\text{DC}}^2}{2}(2J_1(X_1))^2 \cdot 50 \tag{21}$$

$$P(\omega_2) = L(\omega_2)\frac{I_{\text{DC}}^2}{2}(2J_1(X_2))^2 \cdot 50 \tag{22}$$

$$P(\omega_1 \mp \omega_2) = L(\omega_1 \mp \omega_2)\frac{I_{\text{DC}}^2}{2}(2J_1(X_1)J_1(X_2))^2 \cdot 50. \tag{23}$$

B. Experiments

Illustrated in Fig. 5 is a block diagram of the experimental setup. In this experiment, cascading of the interferometric pair MZ1 and MZ2 was accomplished by use of a polarization preserving (PP) fiber. As mentioned earlier, the signals that are actually involved in the mixing are optical signals derived from electrical inputs and are applied to the modulators. To ensure an enhanced mixing efficiency for down-conversion of RF to IF, the optical RF signals should be highly modulated and, therefore, the

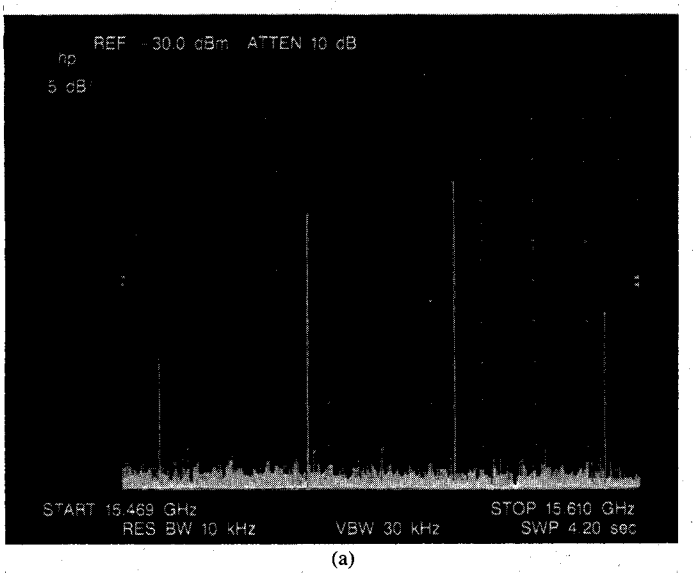

(a)

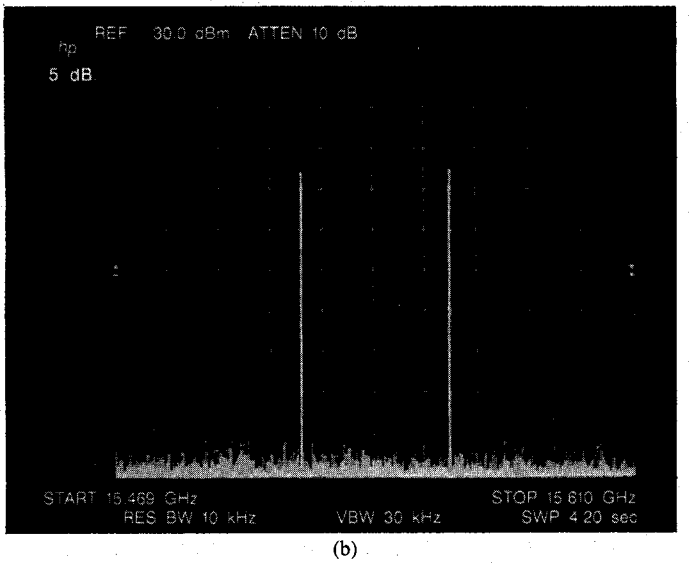

(b)

Fig. 6. Spectrum of drive signals at ≈15.5 GHz: (a) with IM terms and (b) without IM terms.

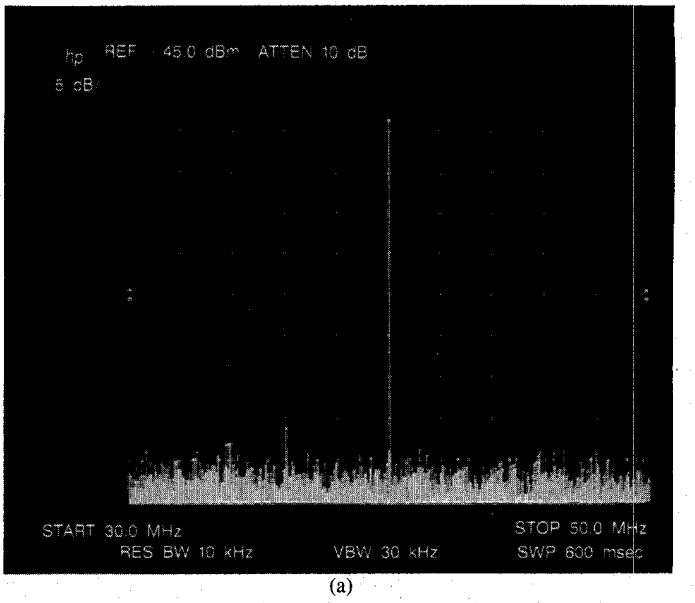

(a)

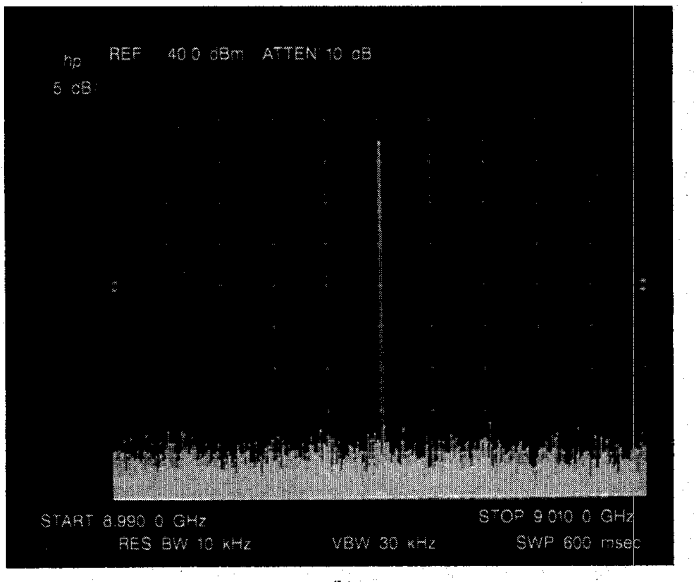

(b)

Fig. 7. Spectrum of difference signal at (a) 40 MHz and (b) 9 GHz.

modulators should be biased at quadrature. If this is not the case, then power is leaked into other frequencies, thereby degrading the mixing efficiency. To demonstrate this, the modulators were biased off-quadrature, and equal amplitude input signals at $f_1 = 15.52$ GHz (RF) and $f_2 = 15.56$ GHz (LO) were applied. The output spectrum, in addition to the signal terms, contains the following beat signals: the desired IF difference signal at $f_2 - f_1 = 40$ MHz and the undesired intermodulation signals at $2f_1 - f_2 = 15.48$ GHz and $2f_2 - f_1 = 15.6$ GHz. This is illustrated in Fig. 6(a) where the spectra of the signal and intermodulation frequencies are shown. However, when each device of the cascaded pair is biased at quadrature, the intermodulation signals disappear, resulting in optical signals at just the signal and difference frequencies. This is illustrated in Fig. 6(b) where just the RF drive signals shown. The spectrum of the corresponding difference signal at 40 MHz is shown in Fig. 7(a). To demonstrate that the IF can be anywhere in the DC to 40 GHz frequency band, we extended the experiment to higher frequencies. If $f_1 = 15$ GHz and $f_2 = 6$ GHz, then the spectrum of the 9 GHz difference signal obtained is shown in Fig. 7(b).

For input signals $f_1 = 15.52$ GHz (RF) and $f_2 = 15.56$ GHz (LO), Fig. 8(a) shows the variation of detected IF power at 40 MHz with input RF power for a detected DC photocurrent of 0.05 mA; the LO pump power was varied from −20 to +20 dBm. As before, since the IF was at 40 MHz, $L(\omega)$ was small and, hence, we neglected. Here, with the LO pump power at +20 dBm, the conversion loss is approximately 66 dB. At 40 GHz, the corresponding computed results are shown in Fig. 8(b) and the conversion loss in this case for a pump power of +20 dBm is about 72 dB. Here, the large conversion loss is attributed in part to the optical insertion loss of the interfero-

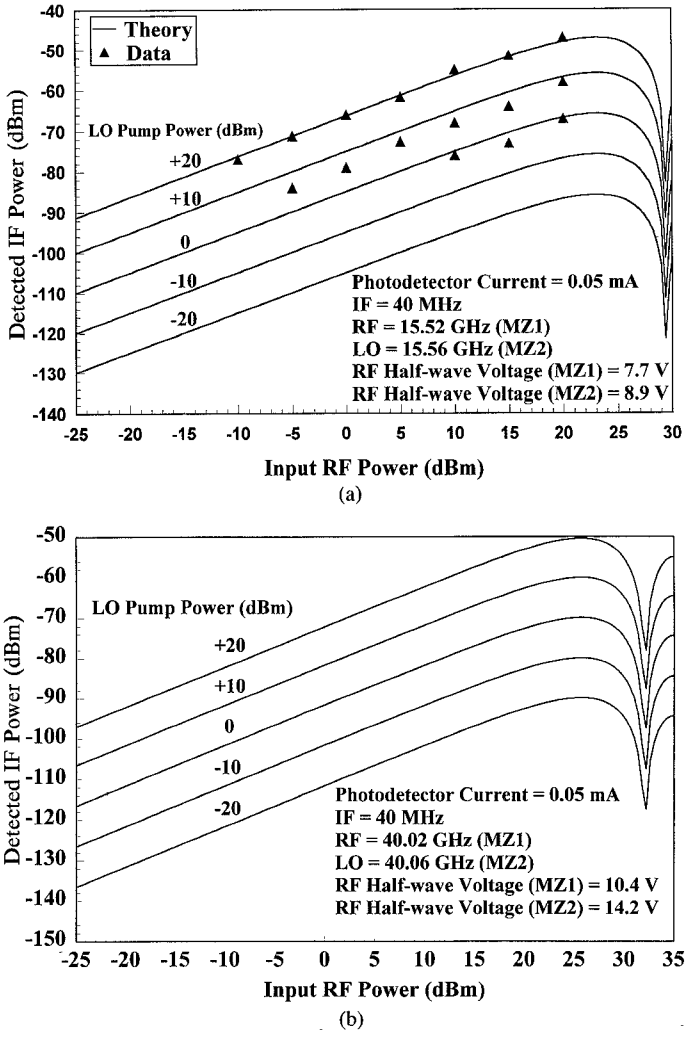

Fig. 8. Performance of the cascaded interferometric pair down-converter biased at quadrature. (a) Modeled and measured response for $f_{RF} \approx f_{LO} \approx$ 15.5 GHz. (b) Modeled response for $f_{RF} \approx f_{LO} \approx$ 40 GHz.

metric pair. We were limited to approximately 12 mW of optical power from the laser at the input to the first modulator. At the output, for a detected DC photocurrent of 0.05 mA, the power striking the detector was 0.1 mW (assuming a detector responsivity of 0.5 A/W) indicating an optical link loss in excess of 20 dB. Here, the modulators biased at quadrature contribute to 14 dB ($\approx$7 dB each) of this loss, and coupling losses account for the rest. The conversion loss of the cascaded interferometric pair would be significantly lower if the power on the photodetector were larger.

The mixing efficiency of the interferometric pair for RF down-conversion is dependent on the strengths of the modulated optical RF and LO signals. It is, therefore, of interest to study optical modulation at the RF and LO signal frequencies. Towards this, we applied two independent equal amplitude signals (one applied to MZ1 and the other to MZ2) spaced 40 MHz apart, to the cascaded interferometric modulator pair biased at quadrature; the frequencies were centered around 15.5 GHz. For the modulating RF input corresponding to MZ1, we show in Fig.

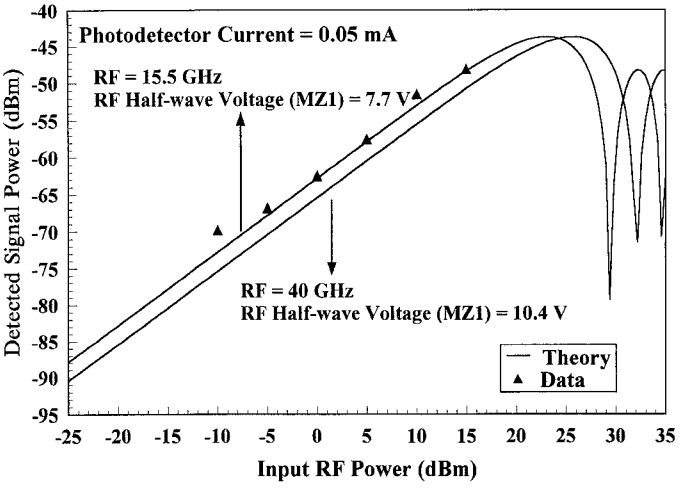

Fig. 9. Response of the interferometric modulator pair at drive frequencies of 15.5 and 40 GHz for equal amplitude drive signals applied to MZ1 and MZ2, respectively.

9 the variation of the detected signal power as a function of input RF power, for a photodetector current of 0.05 mA. For this measurement, $L(\omega) \approx -3$ dB. As shown in Fig. 9, the data is in fairly good agreement with theory with the output increasing linearly with input for power levels that do not cause compression. Also shown, the computed response at 40 GHz assuming the same DC photocurrent and $L(\omega)$. In actuality, however, the signal strength at 40 GHz would be smaller than that predicted in Fig. 9 because $L(\omega)$ would be worse than -3 dB.

VI. Discussion

Microwave-optical mixing in three different configurations of interferometric modulators has been studied. Whereas a single Mach–Zehnder interferometer biased at quadrature can be used to modulate RF signals, an interferometer biased for maximum transmission or the cascaded interferometric pair may be employed for down-conversion. In a typical receiver, since several RF signals are simultaneously received, the study of IMD presented in Section III, is of relevance as it is representative of how the RF signals would interact with each other. In Sections IV and V, we discussed down-conversion of a single RF signal to a lower IF by mixing with an LO. In both these cases, if more than one RF signal is involved, then the analysis presented in Section III may be employed to evaluate mixer performance. The similarity between the discussions presented in Sections IV and V lies in the fact that they both apply to down-conversion of RF to an IF. Compared to the cascaded pair, the drawback of mixing with a single interferometer biased for maximum or minimum transmission is that the RF/LO isolation is limited by the isolation between ports of the power combiner. Also, for applications involving antenna remoting, since just one modulator is involved, there is no question separating the RF and LO portions of the mixer as in the two modulator case.

Compared to conventional microwave mixers, the advantages of using a pair of cascaded interferometers for mixing are its simplicity, port-to-port isolation, and broadband performance. Since the interferometers corresponding to the RF and LO ports are electrically decoupled, there is infinite isolation between these ports. Also, since the generated IF signal is optical, there is no danger of this signal coupling electrically into the RF or LO ports and, hence, the isolation between these ports is also infinite. The modulators themselves exhibit truly broadband performance to 40 GHz, and, hence, the same modulator pair can be used as a mixer anywhere in the DC to 40 GHz span. However, the main problem associated with employing photonics for mixing is the large RF conversion loss. In this context, we note again that the optical LO pump signal in our experiments was derived by applying a large electrical input to the modulator. If this input were further increased, then beyond a certain point, compression of the output would occur. However, with erbium-doped fiber amplifiers (EDFA) currently becoming available at an optical wavelength of 1.5 μm, a better way to generate this optical pump signal would be to employ an EDFA to amplify the optical LO pump signal which could then be mixed with a lower RF signal to accomplish down-conversion. More powerful lasers may also be employed to accomplish the same task.

VII. Conclusions

We have investigated microwave-optical mixing in different configurations of Mach–Zehnder interferometric modulators. It is demonstrated that microwave mixing can be accomplished in the optical domain. We have also presented a novel mixer by cascading a pair of Mach–Zehnder interferometric modulators in series and demonstrate enhanced mixing efficiency by biasing the modulators at quadrature. Some notable advantages of employing photonics for mixing are that the isolation between the individual signal ports is almost infinite, and by virtue of their broadband characteristics, modulators can be employed for mixing anywhere over a 40 GHz frequency span. However, the major drawback of broadband photonic mixing is that the conversion loss is large. But, as modulators with lower half-wave voltages become available, they could be used in conjunction with more powerful lasers and erbium-doped amplifiers to significantly lower the conversion loss.

Acknowledgment

The authors appreciate the efforts of R. W. McElhanon, and A. S. Greenblatt in fabricating the devices and R. D. Esman for loan of microwave equipment and helpful assistance.

References

[1] G. K. Gopalakrishnan, C. H. Bulmer, W. K. Burns, R. W. McElhanon, and A. S. Greenblatt, "40 GHz low half-wave voltage Ti:$LiNbO_3$ intensity modulator," *Electron. Lett.*, vol. 28, no. 9, pp. 826–827, 1992.

[2] D. W. Dolfi and T. R. Ranganath, "50 GHz velocity-matched broad wavelength $LiNbO_3$ modulator with multimode active section," *Electron Lett.*, vol. 28, no. 13, pp. 1197–1198, 1992.

[3] K. Noguchi, O. Mitomi, K. Kawano, and M. Yanagibashi, "Highly efficient 40-GHz bandwidth Ti:$LiNbO_3$ optical modulator employing ridge structure," *IEEE Photonics Technology Lett.*, vol. 5, no. 1, pp. 52–54, 1993.

[4] B. H. Kolner and D. W. Dolfi, "Intermodulation distortion and compression in an integrated electrooptic modulator," *Applied Optics*, vol. 26, no. 17, pp. 3676–3680, 1987.

[5] M. Seino, N. Mekada, T. Yamane, Y. Kubota, and M. Doi, "20 GHz 3 dB bandwidth Ti:$LiNbO_3$ Mach–Zehnder modulator," *ECOC Tech. Dig.*, paper ThG1-5, 1990.

[6] G. K. Gopalakrishnan, W. K. Burns, and C. H. Bulmer, "Electrical loss mechanisms in traveling wave $LiNbO_3$ optical modulators," *Electron. Lett.*, vol. 28, no. 2, pp. 207–209, 1992.

[7] G. K. Gopalakrishnan and W. K. Burns, unpublished data.

[8] R. L. Jungerman, C. Johnsen, D. J. McQuate, K. Salomaa, M. P. Zurakowski, R. C. Bray, G. Conrad, D. Cropper, and P. Hernday, "High-speed optical modulator for application in instrumentation," *IEEE J. Lightwave Technology*, vol. 8, no. 9, pp. 1363–1370, 1990.

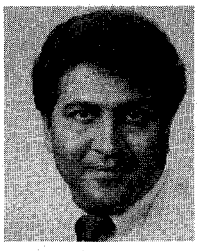

Ganesh K. Gopalakrishnan (S'85–M'90) was born in Madras, India. He received his Ph.D. degree in electrical engineering from Texas A&M University in 1990 and his dissertation research was on microwave-optical interactions in semiconductors.

He is now with Maryland Advanced Development Laboratory at the Optical Techniques Branch of the Naval Research Laboratory, Washington, D.C. His research interests include high-speed integrated optical devices and microwave-optoelectronic circuits and systems.

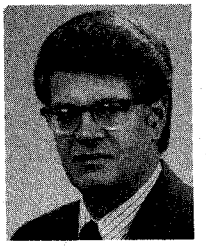

William K. Burns (M'80) was born in Philadelphia, PA, in June 1943. He received the B.S. degree in engineering physics from Cornell University, Ithaca, NY, in 1965, and the M.S. and Ph.D. degrees in applied physics from Harvard University, Cambridge, MA, in 1967 and 1971, respectively. His thesis research was in nonlinear optics.

During 1971, he was a Staff Member at Arthur D. Little, Inc., Cambridge, MA, where he contributed to various laser-related studies and surveys. Since 1972, he has been a Research Physicist at the Naval Research Laboratory, Washington, DC. He is presently Head of the Optical Waveguide Section of the Optical Techniques Branch. His research interests include integrated optics, single-mode fiber optics, and the application of single-mode technology to communications, sensors, and signal processing.

Dr. Burns received NRL's Sigma Xi Award for Applied Science in 1985 and is a Fellow of the Optical Society of America.

Catherine H. Bulmer was born in Kent, England in 1952. She received the B.Sc degree (1st class honors) in electronic engineering from the Robert Gordon's Institute of Technology, Aberdeen, England in 1972, and the Ph.D. degree in electronic engineering from the University of London, England in 1976. Her thesis research was on guided-wave optics.

For fifteen months, she was a Postdoctoral Research Fellow at the IBM Research Laboratory, San Jose, CA, where she was involved in studies of electrochemiluminescence.

Since 1977, Dr. Bulmer has worked in the Optical Techniques Branch of the Naval Research Laboratory, Washington, DC, where her research interests include integrated optics, single-mode fiber optics, and their applications in optical sensing.